

Application of calorimetry on a chip to high-pressure materials

Alexandra Navrotsky^{*†}, Maria Dorogova^{*}, Frances Hellman[‡], David W. Cooke[‡], Barry L. Zink[§], Charles E. Lesher[¶], Juliana Boerio-Goates^{||}, Brian F. Woodfield^{||}, and Brian Lang^{||}

^{*}Thermochemistry Facility and Nanomaterials in the Environment, Agriculture, and Technology Organized Research Unit, and [¶]Department of Geology, University of California, Davis, CA 95616; [‡]Department of Physics, University of California, Berkeley, CA 94720; [§]Department of Physics and Astronomy, University of Denver, Denver, CO 80208; and ^{||}Department of Chemistry and Biochemistry, Brigham Young University, Provo, UT 84602

Edited by Ho-kwang Mao, Carnegie Institution of Washington, Washington, DC, and approved February 7, 2007 (received for review January 23, 2007)

Silicon micromachined calorimeters (“calorimeter on a chip”) are used to measure heat capacities and phase transition enthalpies for thin film, single crystal, and powder samples (5–500 μg). The technology is thus compatible with the small samples produced in multianvil and large diamond anvil cells. Techniques for handling small samples and attaching them to the calorimetric devices have been developed. Initial data illustrate application to CoO and to Fe₂SiO₄ olivine and spinel, a quenched high pressure phase metastable at ambient conditions. The calorimetric entropy of the olivine - spinel transition in Fe₂SiO₄ (−16 ± 5 J/mol·K) is in good agreement with that calculated from phase equilibrium data (−14 ± 3 J/mol·K). A magnetic transition in iron silicate spinel, detected previously by Mossbauer spectroscopy, is seen in the calorimetric signal.

fayalite | Fe₂SiO₄ spinel

Thermodynamic properties of high-pressure phases continue to be important to deep earth geophysics; the focus is shifting increasingly to more complex and higher pressure materials relevant to the lower mantle, D' layer, and core. The effects of aluminum, iron, and other minor constituents on the thermodynamics of silicate spinel, perovskite, and postperovskite phases still are not well known, and magnetic and electronic transitions are not fully characterized.

Much of the difficulty arises from sample size: multianvil experiments produce on the order of 0.5–5 mg of material, whereas diamond anvil cells produce micrograms. Although milligram-sized samples can be studied by oxide melt solution calorimetry to determine their heats of formation (1–2), smaller samples cannot. Conventional adiabatic calorimetry to obtain heat capacities and standard entropies require grams of sample (3). The commercial Quantum Design PPMS system includes the capability to measure heat capacity on samples of 10–100 mg (4). Thus, the entropies of high-pressure materials, especially those that have structural and magnetic transitions, are not well known and remain hard to measure.

“Calorimetry-on-a-chip,” described below, provides heat capacity and phase transition enthalpy data for films and small crystals in the microgram to milligram range. It has been applied, largely by the physics community, mainly to thin films, multilayers, and magnetic materials (5–19). This methodology is now being applied to high-pressure phases, and this report summarizes technique development and early progress and presents data for CoO and the olivine and spinel polymorphs of Fe₂SiO₄.

Initial Studies on CoO and Fe₂SiO₄ Polymorphs

We obtained a single crystal of cobalt oxide whose heat capacity had been measured recently by conventional cryogenic calorimetry at Brigham Young University. This provides a base case for comparison. The 638-μg sample was attached to a thick nitride membrane device (used for measuring large heat capacities) with 183 μg of silver paint. The antiferromagnetic transition is quite well defined (Fig. 1) and its temperature agrees with the adiabatic

measurement to within ≈1 K. This difference is within the precision of the Cernox thermometer. The heat capacities are also in good agreement. The small deviation at lower temperatures is representative of the uncertainty in thermometer calibration and fits within our error bars given this uncertainty.

Having shown the viability of this technique on microgram quantities of material, we turned to measuring the heat capacity of the olivine polymorph of Fe₂SiO₄, fayalite. Attaching a 933 ± 1 μg piece obtained from a sample from the Oak Ridge National Laboratory to a thick nitride membrane device with 180 μg of silver paint, we observed the magnetic transition in fayalite (Fig. 2). The transition appears to be slightly suppressed from that of the large sample studied previously (3). X-ray diffraction discovered that the present sample contained a significant amount of magnetite (Fe₃O₄) contaminant. This may imply oxidizing conditions and the presence of significant concentrations of ferric ion in the olivine phase as well, accounting for the slight suppression and broadening of the magnetic transition. Apart from this difference at the transition, the measured heat capacity is in good agreement with values measured by adiabatic calorimetry on a sample 4 × 10⁴ as large (3). From an integration of the C_p data, we obtain a standard entropy of 148 ± 3 J/mol·K, in good agreement with the literature (3).

Realizing the impurities present in the Oak Ridge sample, we sought a better olivine starting material for spinel synthesis. A sample of well characterized, phase pure and magnetite free Fe₂SiO₄ olivine was provided by D. H. Lindsley (Stony Brook University, Stony Brook, NY). That olivine is more pure and magnetite free than the Oak Ridge material. We did not measure its heat capacity because the full run would take ≈2 weeks and we wished to concentrate on the spinel. Fe₂SiO₄ spinel was synthesized and quenched in a multianvil apparatus and confirmed to be single phase by powder x-ray diffraction. We mounted a few grains of this powder weighing a total of 105 ± 1 μg onto a thick nitride device. We see a clear lambda-type transition at ≈11 K, presumably the Neel transition observed earlier at the same temperature by Mossbauer spectroscopy (20). Table 1 lists heat capacity C_p, enthalpy *H*, and entropy *S* for the spinel phase of Fe₂SiO₄ in the temperature range studied. *H* and *S* are found from the appropriate integrals of C_p, with *H* and *S* set equal to zero at the lowest temperature measured (2.3 K), because the contributions from 0 to 2.3 K are negligible.

Fig. 3 shows the heat capacity of both olivine and spinel Fe₂SiO₄. Between 100 and 300 K, these are essentially the same. The difference in entropy between the two phases at 298 K reflects heat capacity differences below 100 K. Fig. 3 shows that

Author contributions: A.N. and F.H. designed research; M.D., D.W.C., B.L.Z., C.E.L., J.B.-G., B.F.W., and B.L. performed research; D.W.C., J.B.-G., and B.F.W. analyzed data; and A.N. and F.H. wrote the paper.

The authors declare no conflict of interest.

This article is a PNAS Direct Submission.

[†]To whom correspondence should be addressed. E-mail: anavrotsky@ucdavis.edu

© 2007 by The National Academy of Sciences of the USA

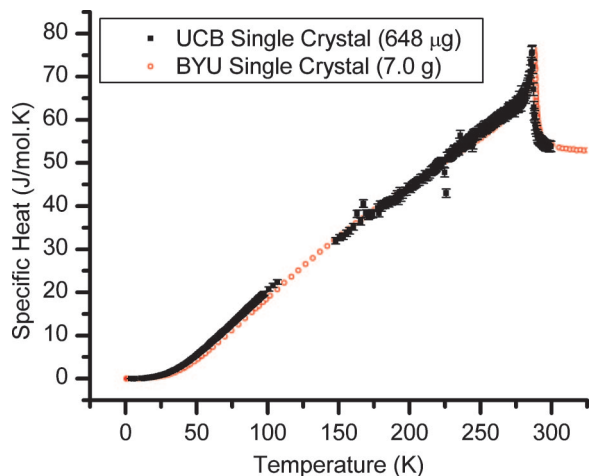


Fig. 1. Comparison of the specific heat of a cobalt oxide (CoO) single crystal measured by our microcalorimeter to that measured at Brigham Young University using cryogenic calorimetry. Errors for the UCB data are shown for all data points and are of order 2%; temperature uncertainty is not shown, but is also of order 1% due to the commercial calibrated thermometer used.

the heat capacity of the spinel phase is higher than that of the olivine below ≈ 15 K; this reflects the Neel transition in the spinel at 11 K. However the olivine heat capacity is higher at 15–100 K, largely due to its antiferromagnetic transition. Fig. 3 *Inset* shows that the entropy of transition becomes roughly constant at -16 ± 5 J/mol·K at 75–300 K. We expect this value to apply to higher temperature as well. This value is in good agreement with the value of -14 ± 3 J/mol·K obtained from an analysis combining phase equilibria and calorimetrically measured enthalpies of transformation (21). The smaller entropy of the spinel is consistent with phase equilibria showing a positive P - T slope for the olivine–spinel transition. Indeed the entropy of the olivine–spinel transition is more negative for Fe_2SiO_4 than for the silicates of Mg, Co, or Ni (21). The difference in magnetic transition behavior between the olivine and spinel forms of iron silicate (Fig. 3) probably accounts for this more negative value. A comparison of the behavior of the heat capacity and magnetic transitions in the olivine and spinel polymorphs of other transition metal silicates and of their solid solutions with the magnesium end-member would be interesting.

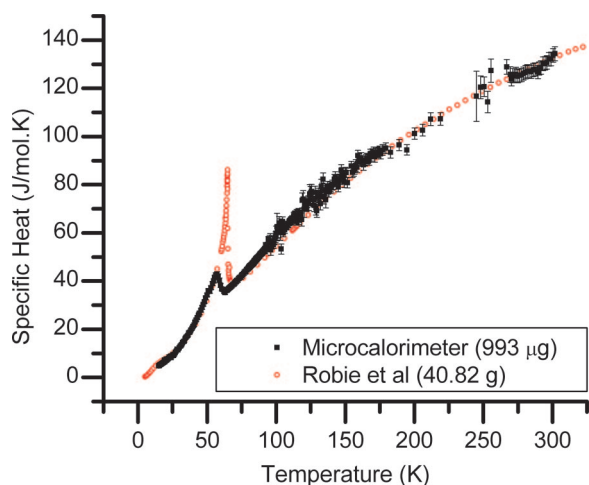


Fig. 2. Comparison of the specific heat of fayalite measured with our microcalorimeters to that measured by Robie *et al.* (3) using cryogenic calorimetry. Error bars are shown at all temperatures for the present data.

Table 1. Tabulated experimental data on Fe_2SiO_4 spinel taken with microcalorimeter

T , K	C_p , J/mol·K	S , J/mol·K	H , J/mol
2.379	0.007 ± 0.004	—	—
5.2	1.09 ± 0.04	0.39 ± 0.03	1.9 ± 0.1
8.2	4.69 ± 0.08	1.69 ± 0.08	11.0 ± 0.5
10.4	8.91 ± 0.07	3.4 ± 0.1	26.7 ± 0.6
11.0	13.27 ± 0.09	4.0 ± 0.1	33.1 ± 0.7
12.5	7.5 ± 0.1	5.3 ± 0.1	48.2 ± 0.8
16.0	6.2 ± 0.2	7.0 ± 0.2	72 ± 1
22.3	5.0 ± 0.4	8.8 ± 0.2	108 ± 3
30	5.2 ± 0.6	10.3 ± 0.4	146 ± 6
35	6.4 ± 0.8	11.2 ± 0.5	180 ± 10
45	10 ± 1	13.4 ± 0.7	270 ± 20
55	17 ± 1	16 ± 1	390 ± 30
65	22 ± 2	19 ± 1	580 ± 50
75	29 ± 2	23 ± 2	840 ± 70
85	37 ± 2	27 ± 2	$1,170 \pm 90$
95	46 ± 2	32 ± 2	$1,600 \pm 100$
105	54 ± 2	36 ± 2	$2,100 \pm 100$
115	63 ± 2	42 ± 2	$2,700 \pm 200$
125	70 ± 2	47 ± 2	$3,300 \pm 200$
135	76 ± 2	53 ± 3	$4,100 \pm 200$
145	82 ± 3	59 ± 3	$4,800 \pm 200$
155	86 ± 3	64 ± 3	$5,700 \pm 300$
165	91 ± 3	70 ± 3	$6,600 \pm 300$
175	94 ± 3	75 ± 4	$7,500 \pm 300$
185	99 ± 3	81 ± 4	$8,500 \pm 300$
195	103 ± 3	86 ± 4	$9,500 \pm 400$
205	106 ± 3	91 ± 4	$10,500 \pm 400$
215	108 ± 3	96 ± 4	$11,600 \pm 400$
225	111 ± 3	101 ± 4	$12,700 \pm 500$
235	115 ± 3	106 ± 4	$13,800 \pm 500$
245	118 ± 3	111 ± 5	$15,000 \pm 500$
255	120 ± 3	116 ± 5	$16,200 \pm 600$
265	121 ± 4	120 ± 5	$17,400 \pm 600$
275	125 ± 4	125 ± 5	$18,600 \pm 600$
285	131 ± 3	129 ± 5	$19,900 \pm 700$
295.067	136 ± 3	134 ± 5	$21,200 \pm 700$

This is a representative data set; the full data set is >500 points. Included are the end points and spline-interpolated, smoothed data in between. A higher density of data is shown at low temperature around the peak in order to more accurately reflect the full data set.

Applications of Calorimetry on a Chip to Mineral Physics

The methodology developed is applicable to a wide variety of materials of interest to the broad mineral physics community. At present, the experiments are conducted at atmospheric pressure so the phases to be studied must be quenchable from high pressure–temperature conditions. Systems for which heat capacities and standard entropies could be determined include (Mg,Fe) silicate spinels and perovskites, including those with substitution by ferric iron and aluminum; Fe_{1-x}O as a function of stoichiometry, including the high pressure nearly stoichiometric material; high-pressure hydrous magnesium silicates, and high pressure phases in silica, zirconia, and titania. Calorimetry of cryogenically quenched high pressure phases, transferred directly onto the detector at low temperature, heat capacities and decomposition enthalpies, analogous to previous work on $\text{Ca}(\text{OH})_2$ (22), could be applied to smaller samples. High-pressure sulfides and alloys of geophysical and planetary significance could be studied. A general survey of magnetic transitions and other phase transitions in iron-bearing high pressure phases between 4 and 500 K would shed light on magnetic and spin behavior. Measurement of thermal conductivity of high pressure

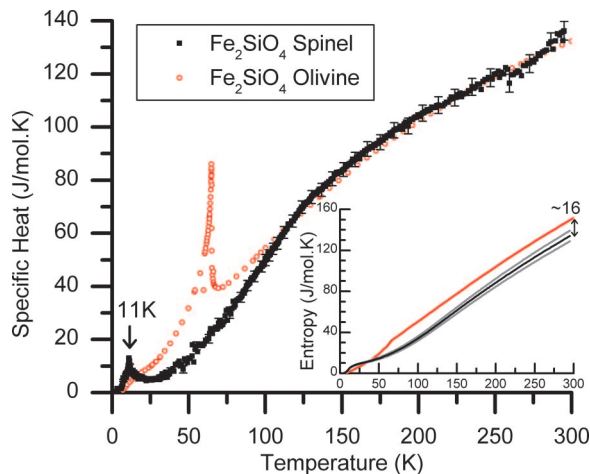


Fig. 3. Comparison of the specific heat of the spinel phase of Fe_2SiO_4 as measured by our microcalorimeters to that of olivine (from ref. 3). (Inset) Entropy for the two samples. Error bars are shown for representative data points for the spinel.

materials might also be possible if sample geometry can be properly controlled. The microfabrication technology used to make these calorimetric measurements could be used for other devices to be placed in high-pressure environments.

As in all low-temperature heat capacity measurements, this technique requires both the calorimetric detector and the appropriate cryostats. The former can be made, usually 10–100 at a time, in a standard microfabrication facility typically associated with materials science and/or electrical engineering research. The latter can be bought or assembled from components. However, calorimetry remains a demanding technique with a somewhat steep learning curve. A complete set of heat capacity measurements at 2–300 K on a given material generally takes ≈ 2 or more weeks. For these reasons, we believe that the methodology will remain limited to a small number of laboratories but that collaboration in terms of identifying interesting problems and materials has the potential to greatly increase the applications to mineral physics.

Recently the commercial Quantum Design PPMS calorimetric system has begun to make an impact of mineralogical research (23–25). It can measure samples in the milligram range and is thus compatible with piston cylinder and larger volume multianvil syntheses. As discussed by Lashley *et al.* (4), accurate measurements using this system also require considerable expertise; no calorimetry is a turnkey operation. We view PPMS and calorimetry on a chip as complementary techniques, with the latter applicable to much smaller samples. Both methods have an attainable accuracy of about ± 1 –2% in heat capacity, good samples and knowledgeable operation being the limiting factors.

While this paper was under review, a paper was published in which the heat capacity of a 24.0-mg sample of Fe_2SiO_4 spinel was measured by using a PPMS system (26). Our data and these are quite similar. Both studies show the magnetic phase transition at 11–12 K. Our value for S_{298} for the spinel is 134 ± 5 J/mol·K, theirs is 140.2 ± 0.4 J/mol·K. It is not clear how their rather small error is estimated; our error estimate may err on the conservative side. The two values are in reasonable agreement. Both studies show that the olivine and the spinel have very similar heat capacities between 150 and 300 K. We stress that our measurements are done on a sample >20 times smaller in mass.

Methodology

Specific heat measurements are based on a Si-micromachined calorimetry device (5–9). These “calorimeters on a chip” (Fig. 4) have been used for both thin films and small bulk samples.

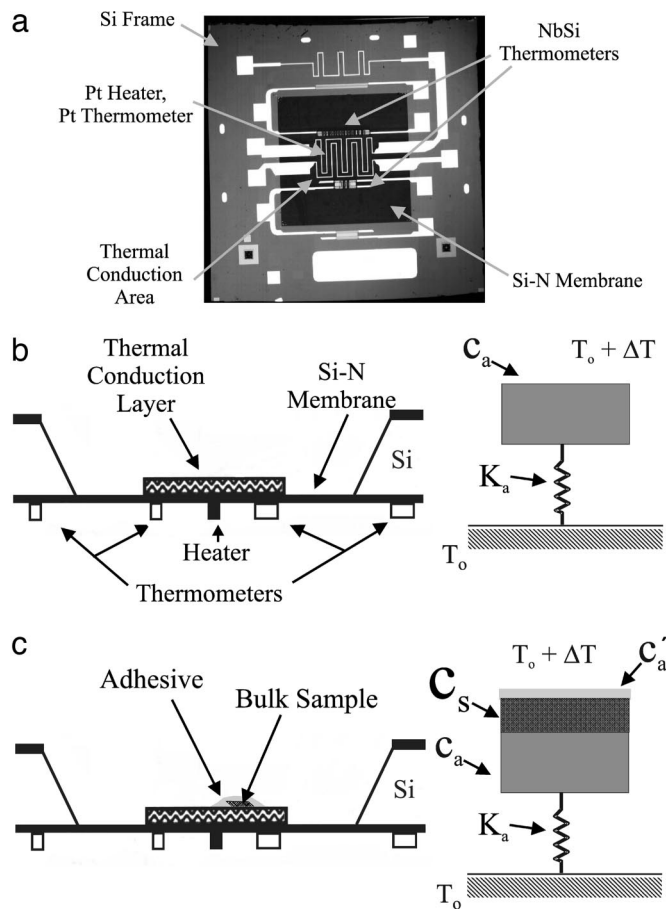


Fig. 4. Calorimetric device. (a) A top view photograph of a device (conduction layer and sample are not visible in this; they are on the back of the membrane). The Pt sample heater, and three sample thermometers are visible in the sample area (Pt and two a-Nb-Si thermometers which differ in R and hence in useful measurement temperature range due to geometry difference in path width and length); matching thermometers are visible on the Si frame area, which is thermally anchored to a copper block. (b and c) Schematic side views of the sample mounting and measurement process. In the analogous electrical circuit, one can think about κ as the electrical conductance, $G = 1/R$, and the heat capacity like a capacitor, C . Similar to an RC circuit, the time constant $\tau = RC = 1/G \times C = C_p/\kappa$.

Different designs have been optimized for different uses, but the heart of the device is a thin (180 nm) 0.5×0.5 cm^2 amorphous Si–N membrane (all components described here are shown and labeled in Fig. 4) supported by a 1×1 cm^2 Si frame. On one side of this membrane, one deposits metal or semiconducting films and uses photolithographic patterning to produce thin film heaters, thermometers, and electrical leads of appropriate resistance and temperature coefficient. On the other side of the membrane, in a 0.25×0.25 cm^2 area at the center, one deposits a thermally conducting material such as gold or copper and then either deposits a thin film sample or uses a thermally conducting adhesive of some type (discussed further below) to attach a bulk sample (shown in the side views of Fig. 4). The thin Si–N membrane provides the necessary thermal isolation of sample from environment while still providing a sample/thermometer platform. On the Si frame are thermometers matching those on the membrane to permit a high sensitivity differential temperature measurement. The devices are metallurgically stable and physically robust under cycling between 2 K and as high as 1000 K and can withstand fairly extensive handling, including photolithographic processing.

Samples are measured by using what is called the relaxation method. In this method, there are two distinct measurement steps. First, the sample heater is turned on and a steady state reached in which the heater power Q equals the heat flowing out via conduction through electrical leads and membrane and via radiation. At this time, the sample thermometer is used to determine a steady state temperature rise ΔT . For small ΔT , in a steady state $Q = \kappa \Delta T$, where κ is an effective thermal link. The second step is to turn the sample heater off and measure the time constant τ of the relaxation of the sample temperature after turning off the sample heater. The total heat capacity (including sample, and all background contributions, commonly referred to as addenda) is then given by $\tau \kappa$. Extracting the sample heat capacity from this total requires a separate determination of the addenda (background) heat capacity, as shown in Fig. 4 *a* and *b* schematically. Further details about the devices and how they are measured can be found in prior publications (5–19).

These devices have been used to measure thin film samples <100 nm thick (weighing <10 μg) below 2 K and 100–500 nm thick (weighing 10–50 μg) up to 525 K in magnetic fields from 0 to 8 T with $\approx 2\%$ absolute accuracy. Even smaller samples can be measured less accurately when information such as an ordering temperature is desired. Because of the nature of the fabrication process, reproducibility of specific heat addenda and of thermal link between sample and environment is very good, varying from device to device by <5%. In most cases, the limit on accuracy is the uncertainty in the thickness of the thin film sample. Relative measurements such as the enthalpy at a phase transition or critical exponent analysis are made with precision better than 0.1% (10–12). Samples measured to date include amorphous magnetic films (*a*-TbFe₂ and giant negative magnetoresistance *a*-Gd-Si alloys) (13, 14), empty and filled fullerenes (C₆₀, K₃C₆₀, C₈₂, LaC₈₂, C₈₄, and Sc₂C₈₄) (15, 16), single crystal and pressed pellets of manganites and ruthenates (10–12), and magnetic and antiferromagnetic multilayered films (Fe/Cr; NiO/CoO, NiO/MgO, CoO/MgO; CoO/SiO₂) (17–19).

We have previously measured powder samples suspended in a liquid and dropped onto devices (15, 16) and have also successfully measured small single crystals or other bulk samples (200–500 μg) thermally anchored to thick membrane devices by using indium to attach the samples (10–12). The application to high pressure samples, however, requires significant modification of procedures. The indium requires physical pressure, which is incompatible with the thinner membranes needed for small (<100 μg) samples. Moreover, possible decomposition of metastable high-pressure materials makes it undesirable to heat the device to melt the indium to attach samples. The wide temperature range desired makes conducting grease (commonly used in the literature for low temperature measurements) a poor option, because grease has large and thermal history-dependent, hence irreproducible, heat capacity between 77 K and room temperature. Our first attempt to use gallium (which has a lower melting point) to replace the indium was unsuccessful due to poor wetting characteristics of Ga on the oxide samples, as opposed to good wetting on metals. Therefore, we turned to and have developed the use of silver paint, manufactured by SPI Supplies (West Chester, PA), which has previously been used to attach electrical leads to samples. This paint can be diluted with butyl acetate to a useful consistency to attach samples.

After placing the sample (one or more small crystals of known mass) on the center of the thermal conduction layer, the diluted silver paint is dropped onto the sample and allowed to dry overnight in a vacuum desiccator. We have measured the mass of the resulting system over a period of days after this process, and find an initial rapid decrease as the solvent evaporates, which is reduced to <1% per day after 24 h.

Once the butyl acetate solvent has evaporated, the resulting thin layer of paint holds the sample securely. Silver paint is designed and experimentally found to give good electrical contact, so its thermal conductivity is also expected to be high. The relaxation method used for measurement directly shows whether this thermal contact is good or not, as good thermal contact yields a single exponential decay, whereas poor thermal contact would show the classic double exponential “tau 2” effect. We have verified that the resulting thermal decays of the relaxation method are that of a single time constant, justifying our assumption of the paint providing good thermal contact between sample and calorimeter. This approach to mounting samples thus provides an avenue for measuring metastable bulk samples with small mass.

We find that silver paint has a moderate heat capacity over the entire temperature range, more than that of bulk silver, presumably because the bonding agent gives a significant contribution, but less than (and more reproducible than) that of grease. This addenda contribution is consistent per bottle of silver paint, but we did see deviations between bottles. The contribution is determined from the measured mass of the silver paint. The uncertainty in this mass (measured to $\pm 1 \mu\text{g}$) is the largest contribution to the random error in this technique.

The errors given in this paper are representative of estimated experimental accuracy and are dominated primarily by the systematic error in our technique (discussed in ref. 8), plus absolute temperature calibration uncertainty, which could be improved. The agreement with adiabatic data for CoO and fayalite as well as additional 2D heat flow simulation work (26) also suggest systematic errors of similar magnitude. Other primary sources of error are (for the samples shown here, which are large for this technique) are the uncertainty in silver paint mass and error in the decay time fit. Smaller errors are associated with the scatter and fitting errors in κ , the uncertainty in the addenda measurement, and the small uncertainty in sample mass.

For the data shown here, an estimate of absolute accuracy was made as follows. Previous experiments and simulations give a systematic error of <2% (8, 26). The agreement with adiabatic data for CoO and fayalite also suggest systematic errors of similar maximum magnitude. The error bars shown are calculated by adding in quadrature the following: 2% of the total C_p (due to systematic error in technique), $1 \mu\text{g} \times \mu\text{g}$ sample mass $\times C_p$ (error due to $\pm 1 \mu\text{g}$ uncertainty of sample mass), $1 \mu\text{g} \times C_p$ of Ag paint (error due to uncertainty in Ag paint mass), κ times the error in τ (error due to τ fit), and τ times the error in κ (calculated via 98% confidence bands in various polynomial fits). The error in κ fit is small (0.1–0.3%). The error in τ fit is on the order of 0.2–1%. There is also a <1% uncertainty in temperature due to thermometer calibration. Propagating all these errors suggests that an absolute accuracy on the order of 2% in heat capacity, dominated by the systematic errors discussed above, is attainable.

For 10- to 100- μg samples, it is necessary to use the standard thin membrane (180 nm thickness) devices to keep the background heat capacity addenda small. For larger samples (100–900 μg), the thicker membrane (1.5 μm) devices work well. Samples >1 mg are not well measured with these calorimeters on a chip due to the long time constants involved; for these samples, the PPMS system (4, 23, 24) provides a possible choice.

We thank J. Chen, D. H. Lindsley (State University of New York, Stony Brook, NY) and J. Post (Smithsonian Institution, Washington, DC) for samples. This work received support from COMPRES, the Consortium for Materials Properties Research in the Earth Sciences, and by National Science Foundation Grant EAR-0229332 and the U.S. Department of Energy, Office of Basic Energy Sciences, Materials Sciences and Engineering Division, under Contract DE-AC02-05CH11231. The adiabatic calorimetry on CoO at Brigham Young University was supported by U.S. Department of Energy Grant DE-FG02-05ER15666.

1. Navrotsky A (1997) *Phys Chem Min* 24:222–241.
2. Ito E, Akaogi M, Topor L, Navrotsky A (1990) *Science* 249:1275–1278.
3. Robie RA, Cabell BF, Hemingway BS (1982) *Am Mineral* 67:463–469.
4. Lashley JC, Hundley MF, Migliori A, Sarrao JL, Pagliuso PG, Darling TW, Jaime M, Cooley JC, Hults WL, Morales L, et al. (2003) *Cryogenics* 43:369–378.
5. Denlinger DW, Abarra EN, Allen K, Rooney PW, Messer MT, Watson SK, Hellman F (1994) *Rev Sci Instr* 65:946–959.
6. Zink BL, Revaz B, Sappey R, Hellman F (2002) *Rev Sci Instr* 73:1841–1844.
7. Zink B, Hellman F (2004) *Sol St Comm* 129:199–204.
8. Revaz B, O'Neil D, Hull L, Hellman F (2003) *Rev Sci Instr* 74:4389–4403.
9. Revaz B, Zink BL, Hellman F (2005) *Thermochim Acta* 432:158–168.
10. Kim D, Revaz B, Zink BL, Hellman F, Mitchell JF, Rhyne JJ (2002) *Phys Rev Lett* 89:227202/1–227202/4.
11. Kim D, Zink BL, Hellman F, Coey JMD (2002) *Phys Rev B* 65:214424/1–214424/7.
12. Kim D, Zink BL, Hellman F, McCall S, Cao G, Chow JE (2003) *Phys Rev B* 67:100406/1–100406/4.
13. Hellman F, Abarra EN, Shapiro, A. L., van Dover RB (1998) *Phys Rev B* 58:5672–5683.
14. Zink BL, Janod E, Allen K, Hellman F (1999) *Phys Rev Lett* 83:2266–2269.
15. Allen K, Hellman F (1999) *J Chem Phys* 111:5291–5294.
16. Allen K, Hellman F (1999) *Phys Rev B* 60:11765–11772.
17. Revaz B, Cyrille M-C, Zink B, Schuller IK, Hellman F (2002) *Phys Rev B* 65:094417/1–094417/8.
18. Abarra EN, Takano K, Hellman F, Berkowitz AE (1996) *Phys Rev Lett* 77:3451–3454.
19. Tang YJ, Smith DJ, Zink BL, Hellman F, Berkowitz AE (2003) *Phys Rev B* 67:054408/1–054408/7.
20. Suito K, Tsutsui Y, Nasu S, Onodera A, Fujita FE (1984) *Mat Res Soc Symp Proc* 22:295–298.
21. Navrotsky A (1987) *Prog Solid State Chem* 17:53–86.
22. Schoenitz M, Navrotsky A, Leinenweber K (2000) *Phys Chem Min* 27:604–609.
23. Cemic L, Dachs E (2006) *Phys Chem Min* 33:457–464.
24. Dachs, E. Geiger CA (2006) *Am Mineral* 91:894–906.
25. Dachs E, Bertoldi C (2005) *Eur J Mineral* 17:251–261.
26. Yong W, Dachs E, Withers AC, Essene EJ (2007) *Phys Chem Min* 34:121–127.